Journal of Applied Electrochemistry **30**: 929–937, 2000.

Corrosion protection of steel in molten Li_2CO_3–K_2CO_3 and Na_2CO_3–K_2CO_3 mixtures in a hydrogen-containing atmosphere

I.M. PETRUSHINA, L. QINGFENG, F. BORUP and N.J. BJERRUM*
Department of Chemistry, Technical University of Denmark, DK-2800 Lyngby, Denmark
*(*author for correspondence)*

Received 22 February 1999; accepted in revised form 30 November 1999

Key words: corrosion protection, fuel cells, hydrogen-containing atmosphere, molten carbonates, nitride coatings, voltammetry

Abstract

The electrochemical behaviour of TiN-, TiN–AlN-, Cr- and CrN-coated 316L stainless steel in molten Li_2CO_3–K_2CO_3 and Na_2CO_3–K_2CO_3 melts in a reducing gaseous atmosphere (10% H_2–90% N_2) was studied using voltammetry and scanning electron microscopy combined with energy-dispersed X-ray analysis in the temperature range of 600–730 °C. To facilitate the identification of the electrochemical reactions the voltammetric behaviour of stainless steel, titanium, nickel and gold was also investigated. Voltammetric characteristics obtained at AlN–TiN coated electrodes showed no anodic reactions at potentials more negative than that of CO_3^{2-} oxidation. Cr- and CrN-coated electrodes demonstrated a suppressed anodic dissolution after the first steady state voltammetric cycle. The voltammograms obtained for the other electrodes studied displayed the corresponding anodic metal-dissolution waves. TiN, AlN, Cr and CrN coatings seem to be the most promising as corrosion-resistant materials for the anodic compartments of molten carbonate fuel cells.

1. Introduction

Corrosion of metal separator plates in molten carbonate melts is one of the main problems in molten carbonate fuel cell (MCFC) technology [1]. This problem is most complicated in the reducing atmosphere of the anode compartment. Thus, optimization of stainless steel composition and development of protective coatings are important to the further development of MCFC technology.

It has been found previously that the addition of metals such as Zr, Ti or Al increases the oxidation resistance of steels in molten carbonate media [2–4]. Stainless steel was also protected by coating with layers of Al, Cr, Ni or an alloy of these metals followed by heating in an oxidizing atmosphere to form an Al–Fe–Cr–Ni oxide surface layer [5–7].

Plasma vapour deposited TiN is known to have high corrosion resistance and low electrical resistance [8]. The peculiarity of this type of protective layer is that it undergoes at least partial oxidation when exposed to corrosive media. It should therefore rather be treated as an oxide-containing protective layer [9]. Surface analyses have shown that the TiN coating is oxidized in aqueous media with formation of TiO_2, titanium suboxides and titanium oxonitride [10, 11]. This partially oxidized surface layer exhibits higher adherence to a steel surface and higher corrosion resistance than TiO_2 coatings [10]. This behaviour has been attributed to the presence of the TiN interlayer between titanium oxide upper layer and stainless steel surface.

The goal of our investigation was to test a new procedure for producing Ti, Cr and Al oxide protective coatings starting from nitride coatings. These layers were expected to confer better corrosion resistance than oxides obtained by direct oxidation of the studied metals. This approach was based on the assumption that titanium, aluminium and chromium nitrides should be less stable thermodynamically than the corresponding oxides in the molten alkali metal carbonates [12, 13]. Consequently, after contact with the molten carbonates, nitrogen in the nitrides will be exchanged for oxygen. It is possible that after this exchange N atoms will diffuse inside the stainless steel support, reducing the interface tension and improving the adhesion between the stainless steel support and surface oxide layer. Preliminary corrosion tests with TiN-, TiAlN- and Cr-coated stainless steel under the reducing atmosphere have shown remarkable corrosion resistance [14, 15]. These results were subsequently confirmed by Keijzer et al. for a TiN/Ti_2N coating after corrosion tests in molten Li_2CO_3–K_2CO_3 in a reducing (anodic) atmosphere [16, 17]. It has also been shown [17] that this coating is less stable in an air/CO_2 atmosphere (cathodic conditions) and after 24 h under these corrosion conditions it transforms into three surface layers: an upper layer of

$LiFeO_2$, a Ti-rich interlayer and a bottom layer of Cr–Fe-oxide.

In the present work the corrosion behaviour of stainless steel protected with TiN, $TiAlN_2$ or CrN surface layers in molten Li_2CO_3–K_2CO_3 and Na_2CO_3–K_2CO_3 mixtures at 600–730 °C was studied using voltammetric measurements, scanning electron microscopy (SEM) and energy-dispersed X-ray diffraction (EDX). Steady-state voltammetry was used as the main test of corrosion stability, because there is a clear correlation between the resistance to forced anodic dissolution of a material over a wide potential range and the corrosion resistance of that material. Taking into account that the coatings studied were plated on stainless steel, the voltammetric behaviour of these coatings was compared with the electrochemical behaviour of the stainless steel itself and some of its components (Cr, Ni). This helped to eliminate the anodic waves for stainless steel in the voltammograms. It was also important to eliminate the waves for the electrolyte in the voltammograms. They were therefore compared with the voltammograms for gold in the same electrolyte. It was also interesting to compare the electrochemical behaviour of CrN and TiN with the electrochemical behaviour of Cr and Ti. Fortunately, there is a large amount of published data on the steady-state voltammetry of the above-mentioned traditional materials for molten carbonate fuel cells [1, 2, 18, 20, 21]. To make the most precise comparison, the voltammetric measurements with these traditional materials were repeated in the same melts and under the conditions studied. However, there was no need for an in-depth electrochemical investigation of stainless steel, nickel, chromium, titanium and gold in the carbonate melts employed, and published data were used to identify the voltammetric waves.

2. Experimental details

Materials used for preparation of alkali carbonate melts were Li_2CO_3 (Heraeus >99%), Na_2CO_3 (Heraeus >99%) and K_2CO_3 (Heraeus >99%). The eutectic mixture of Li_2CO_3–K_2CO_3 (62–38 mol %) and a Na_2CO_3–K_2CO_3 mixture (62–38 mol %) were used as electrolytes. The investigation was performed in a reducing gas atmosphere (10 vol % hydrogen–90 vol % nitrogen) so as to reproduce the corrosion conditions in the vicinity of the molten carbonate fuel cell anode. The inlet gas was humidified by bubbling it through water at 25 °C before introducing it into the cell. At this temperature the equilibrium content of water in the gas flow should be 3.12 vol %. The outlet gas was led through a trap to prevent entry of air. Most of the measurements in the Li_2CO_3–K_2CO_3 melt were performed at 650 °C. Measurements in the Na_2CO_3–K_2CO_3 melt were conducted at 730 °C.

The cell for the electrochemical experiments is shown in Figure 1. The working electrodes were made from

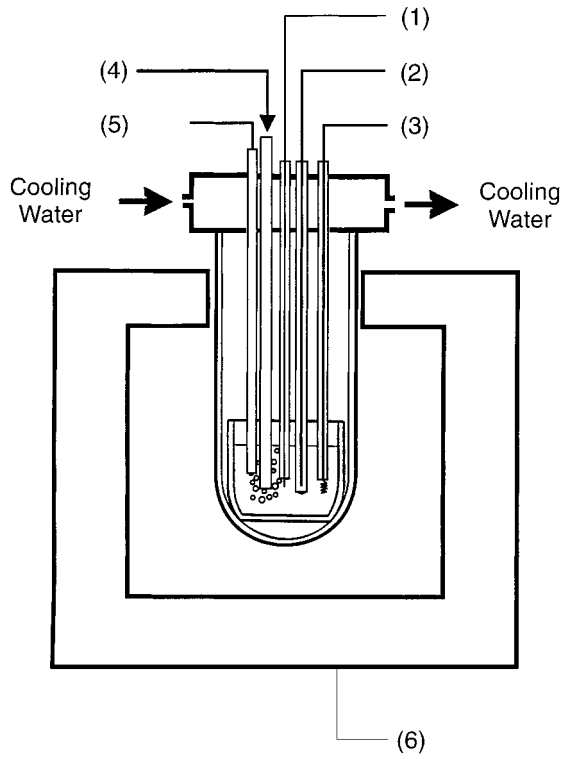

Fig. 1. Electrochemical cell: (1) working electrode; (2) reference electrode; (3) counter electrode; (4) gas inlet; (5) thermocouple, (6) furnace.

metal wires (dia. 2 mm) protected by alumina tubes. The working area was 0.5 cm^2. The metals tested included nickel (Inco, FM-61), stainless steel (316L), titanium (Goodfellow T1007910) and gold (99.99% pure). TiN, TiN–AlN, Cr and CrN protective layers (2.1 μm thick) were coated onto stainless steel wires (316L) by the physical vapour deposition (PVD) technique (unbalanced magnetron sputtering) employing equipment from Chemicon (type CHEMICON CC800). The counter electrode was made of gold wire (99.99% pure) in the form of a spiral. The silver reference electrode was placed in an alumina tube with a small hole in the bottom and with a dry air atmosphere. A 0.1 M solution of Ag_2SO_4 in the Li_2CO_3–K_2CO_3 (62–38 mol %) melt was used as the electrolyte for the reference electrode. According to [2] the equilibrium potential of the Ag^+/Ag electrode vs the more common $O_2,CO_2/CO_3^{2-}$ reference electrode is approximately −0.08 V. All potentials mentioned below are relative to the Ag^+/Ag reference electrode.

The electrochemical measurements were performed with a potentiostat/galvanostat (Autolab–PGSTAT20, Eco Chemie), controlled by a computer. The techniques used were steady-state voltammetry and cyclic voltammetry. All voltammetric experiments were carried out after several hours of stabilization of the corrosion potential of the working electrode.

The corrosion experiments were performed with TiN-coated stainless steel samples in Li_2CO_3–K_2CO_3 (62–38 mol %) and Na_2CO_3–K_2CO_3 (62–38 mol %) melts

under the H_2/N_2 atmosphere at 650 °C and 730 °C, respectively. The time of exposure to corrosion for all the samples was always 24 h. The TiN coating was examined before and after the corrosion test using SEM (Philips SEM S 05 microscope) in combination with energy-dispersed X-ray analysis (EDAX 9900 analyser).

3. Results and discussion

3.1. *Anodic limiting reactions*

The results of the cyclic voltammetry and steady-state voltammetry measurements on gold in the Li_2CO_3–K_2CO_3 melt are shown in Figures 2–4. In the present corrosion study, gold was chosen as a corrosion-stable reference material [2]. Owing to the corrosion stability of gold, the voltammetric characteristics of this electrode should reflect only the electrochemical activity of the electrolyte. This will help to separate the electrochemical reactions due to the electrolyte from those due to the electrode materials for the less corrosion-stable materials. Indeed, it can be seen from Figure 2 that the limiting anodic reactions (waves Ox_1 and Ox_2 in Figure 2) begin at potentials more negative than the Au/Au^{3+} standard potential [2] (0.49 V). This means that only the electrolyte components participate in these reactions. Analyses of the published data and standard potential values [2] show that wave Ox_1 can be ascribed to an oxidation of the carbonate-anion:

$$CO_3^{2-} \rightarrow CO_2 + \frac{1}{2}O_2 + 2e^- \quad (1)$$

However, taking into account the presence of water and OH^- ions in the melt, this could probably also be caused by OH^- oxidation:

$$2\,OH^- \rightarrow \frac{1}{2}O_2 + H_2O + 2e^- \quad (2)$$

This is substantiated by the data presented in [2].

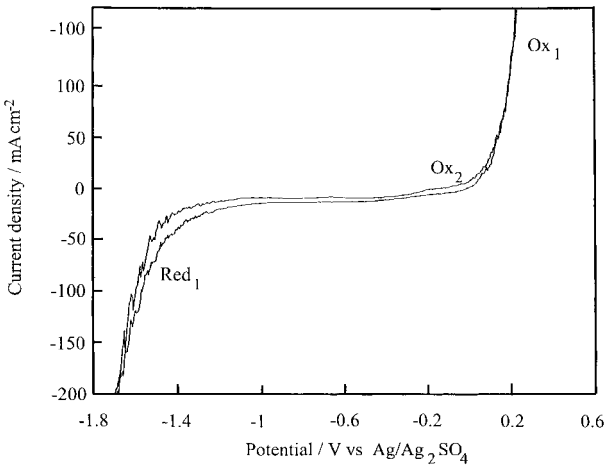

Fig. 2. Cyclic voltammetric curve for Au in molten Li_2CO_3–K_2CO_3 eutectic electrolyte at 650 °C and 10 mV s^{-1} in a reducing atmosphere (10% hydrogen–90% nitrogen).

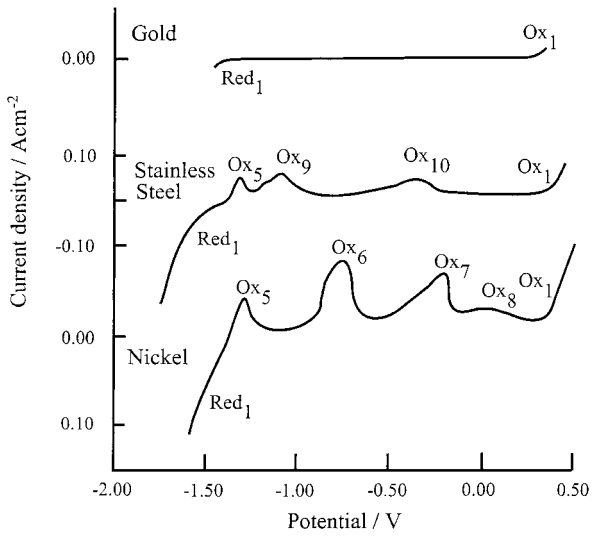

Fig. 3. Steady-state voltammetric curves obtained for gold, stainless steel (316L) and nickel electrodes in molten Li_2CO_3–K_2CO_3 eutectic electrolyte at 650 °C and 1 mV s^{-1} (1st run) in a reducing atmosphere (10% hydrogen–90% nitrogen).

It can be seen from Figures 2–4 that the potential of wave Ox_1 depends on the nature of the working electrode material, and varies between 0.2 and 0.3 V for gold, nickel, stainless steel, TiN and TiN–AlN. The data presented in Figure 4 show no anodic limiting reaction at the titanium electrode in the positive potential range studied. These data are consistent with the results obtained by Chauvaut et al. [18, 24] on the electrochemical behaviour of Ti electrodes in molten Li, Na/CO_3. This behaviour of the Ti electrodes under

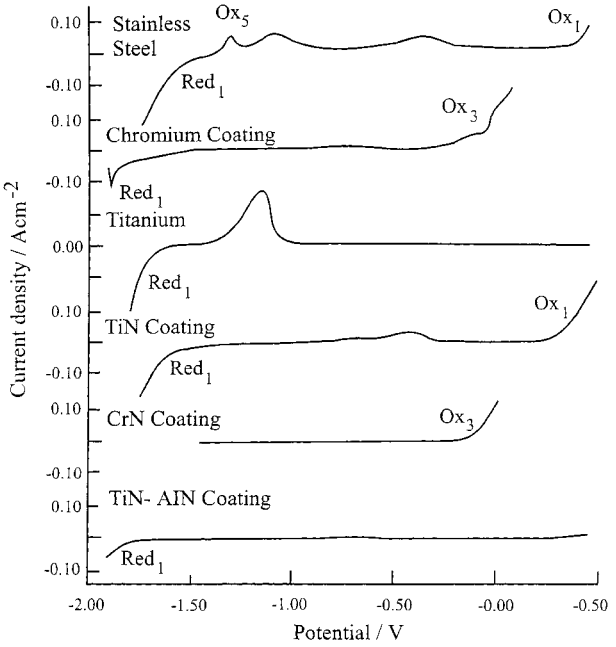

Fig. 4. Steady-state voltammetric curves obtained for stainless steel (316L) and Ti and Cr–, TiN-, CrN-, TiN–AlN- coated stainless steel electrodes in Li_2CO_3–K_2CO_3 eutectic electrolyte at 650 °C and 1 mV s^{-1} (1st run) in a reducing atmosphere (10% hydrogen–90% nitrogen).

conditions of high positive polarization can be ascribed to the formation of an oxide surface layer at which CO_3^{2-} is electrochemically inactive. Similar anodic behaviour of titanium electrodes has also been observed in molten alkali metal acetates and alkali thiocyanates [19].

The voltammograms obtained at Cr- and CrN-coated stainless steel are shown in Figures 4–6. It can be seen from Figure 5 that when the Cr-coated electrode is cycled between −2.0 V and 0.5 V, there are two anodic peaks, Ox_3 and Ox_4, at potentials more negative than for CO_3^{2-} oxidation at the first cycle. However, the waves Ox_3 and Ox_4 decrease significantly during the next voltammetric cycles. Similar behaviour, but with only one wave (Figure 6, wave Ox_3), is found for the CrN-coated stainless steel electrode.

According to Vossen et al. [20], the potential window with the Li_2CO_3–K_2CO_3 melt for a chromium electrode is anodically limited by one of the following two reactions proceeding at potentials close to −0.5 V (vs the CO_2/O_2 reference electrode):

$$LiCrO_2 + 2\,CO_3^{2-} \rightarrow CrO_4^{2-} + 2\,CO_2 + Li^+ + 3\,e^- \quad (3)$$

or

$$Cr + 4\,CO_3^{2-} \rightarrow CrO_4^{2-} + 4\,CO_2 + 6\,e^- \quad (4)$$

The latter reaction proceeds at −0.5 V (vs the CO_2/O_2 reference electrode) and more anodic potentials. The reaction Ox_4 is absent at the CrN-coated electrode (Figure 6), and we can therefore assume the occurrence of electrochemical oxidation of chromium (similar to Reaction 4). The electrochemical behaviour of Cr- or CrN-coated electrodes during cycling (Figures 5 and 6) is, however, due to passivation of these surface layers rather than to their complete electrochemical dissolution according to Reactions 3 and 4 (compare Figures 5–7).

The difference in the anodic behaviour of the Ti electrode and the TiN-coated steel electrode (Figures 3 and 4) can be explained by the difference in the nature of protective layers at the surface of these electrodes.

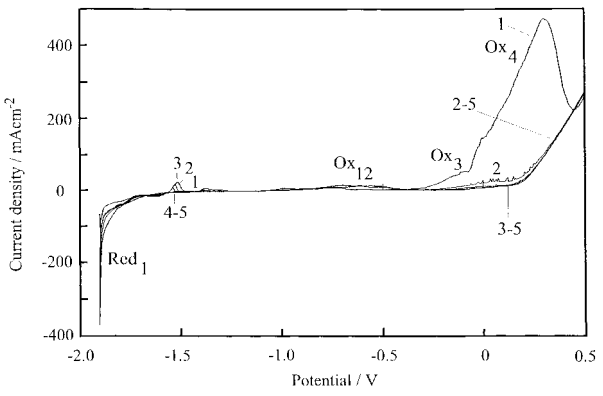

Fig. 5. Steady-state voltammetric curves obtained for Cr- coated stainless steel (316L) electrodes in Li_2CO_3–K_2CO_3 eutectic electrolyte at 650 °C and 1 mV s^{-1} (1st–5th runs) in a reducing atmosphere (10% hydrogen–90% nitrogen).

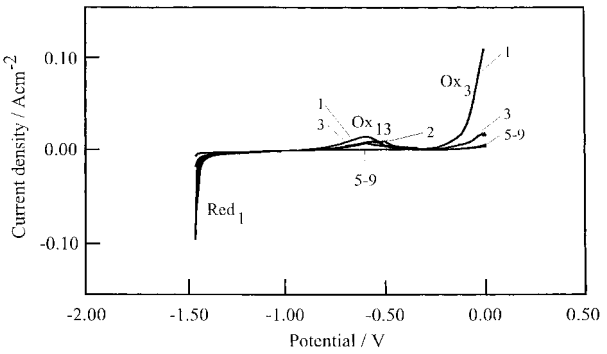

Fig. 6. Steady-state voltammetric curves obtained for the CrN-coated stainless steel electrode in Li_2CO_3–K_2CO_3 eutectic electrolyte at 650 °C and 1 mV s^{-1} (1st–9th runs) in a reducing atmosphere (10% hydrogen–90% nitrogen).

3.2. *Cathodic limiting reactions*

The cathodic limit (Figures 2 and 3, wave Red_1) in the voltammograms obtained at the Au electrode in the Li_2CO_3–K_2CO_3 melt was about −1.1 V. The electrochemical reduction of the CO_3^{2-}-ion has been shown to be the limiting cathodic reaction at the gold electrode in the lithium-containing carbonate melts in CO_2/O_2 or Ar atmospheres [2]:

$$CO_3^{2-} + 4\,e^- \rightarrow C\downarrow + 3\,O^{2-} \quad (5)$$

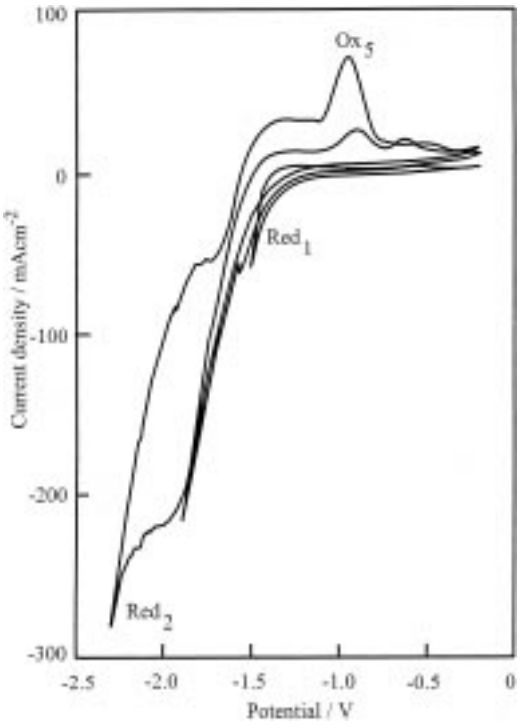

Fig. 7. Cyclic voltammetric curves obtained for the Au electrode in Li_2CO_3–K_2CO_3 eutectic electrolyte at 650 °C and 200 mV s^{-1} in a reducing atmosphere (10% hydrogen–90% nitrogen).

According to [2], however, Reaction 5 starts at −1.82 to −2.02 V (vs the Ag^+/Ag reference electrode) in the acidic (i.e., high partial pressure of CO_2) molten carbonates and at even more negative potentials in the basic electrolytes.

Taking into account the published data on the standard potential of the hydrogen electrode in molten carbonates [2] (−0.98 V vs Ag^+/Ag) and the $H_2/N_2/H_2O$ atmosphere in the electrochemical cell, one can assume that Red_1 is an electrochemical reduction of water according to one of the following equations:

$$H_2O + 2e^- \rightarrow H_2 + O^{2-} \quad (6)$$

or

$$H_2O + CO_2 + 2e^- \rightarrow H_2 + CO_3^{2-} \quad (7)$$

This assumption is consistent with voltammetric data presented in Figure 7. It can be seen that wave Red_1 can be run over at high cathodic current densities, and that a new cathodic limiting wave Red_2 can be obtained. This wave starts at a potential more negative than −2.0 V, that is, it is definitely more likely to be due to Reaction 5. It can also be seen from Figure 7 and 8 that wave Ox_5 is clearly due to the electrochemical oxidation of the products of Reaction 6 (or 7), i.e. an oxidation of hydrogen in the direction opposite to that of Reaction 6 (or 7).

For nickel, titanium, stainless steel and Cr-, TiN-, CrN-, AlN-TiN-coated stainless steel, the cathodic limiting reaction potentials vary in the region from −1.0 V (Ni) to −1.9 V (Cr) (Figures 3 and 4). However, this potential range is still more positive than potentials for the CO_3^{2-} reduction [2]. It can therefore be assumed that reaction Red_1 for all the electrode materials studied is reduction of water with formation of hydrogen (Reactions 6 and 7). The potential and the reversibility of this reaction clearly depend on the catalytic activity of the electrode material. It can be seen from Figure 8 that nickel (curve 1) is a better catalyst for water reduction (wave Red_1, Equations 6 and 7) and hydrogen oxidation (wave Ox_5, Reaction 7 (reversed)) than stainless steel (curve 2).

It is important to note that the cathodic behaviour is different for Cr- and CrN-coated electrodes (Figures 3–6), indicating the difference in the nature of the surface protective layers for the Cr and CrN coatings.

3.3. *Anodic dissolution of metals*

The anodic waves obtained at the electrode materials examined, inside the electrolyte potential window, can be ascribed mainly to the anodic dissolution of these materials with the formation of passive oxide layers [1, 2, 18–22] (Figures 3, 4, 8, 9). For nickel, waves Ox_7 and Ox_8 (Figure 3) can be ascribed to the following reactions [1]:

$$Ni + CO_3^{2-} \rightarrow NiO + CO_2 + 2e^- \quad (8)$$

and

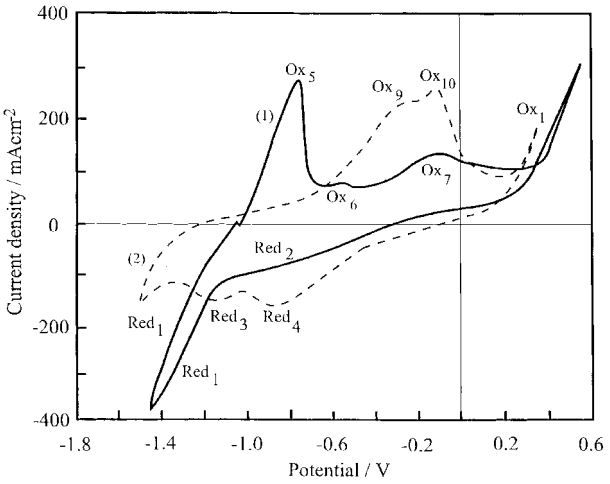

Fig. 8. Cyclic voltammetric curves obtained for the (1) Ni and (2) stainless steel (316L) electrodes in Li_2CO_3 atmosphere-K_2CO_3 eutectic electrolyte at 650 °C and 50 mV s^{-1} in a reducing (10% hydrogen–90% nitrogen).

$$Ni \rightarrow Ni^{2+} + 2e^- \quad (9a)$$

$$Ni^{2+}_{NiO} \rightarrow Ni^{3+}_{NiO} + e^- \quad (9b)$$

This assumption is based on the fact that the initial potentials of the waves Ox_7 and Ox_8 are more positive than the standard potentials for Reactions 8 and 9 (−0.731 V and −0.707 V vs Ag^+/Ag, respectively). It can be seen from Figures 3 and 8 that wave Ox_6 increases as the potential scan rate decreases, and that wave Ox_6 appears only after the potential scan is reversed after the electrochemical reduction of water (Figure 9, wave Red_1). It may therefore be assumed that reaction Ox_6 is an electrochemical dissolution of nickel hydride or hydrogen dissolved in nickel [23]. It is also apparent from Figure 9 that the wave Red_2 corresponds to reduction of the oxide layer which is formed during the nickel oxidation (wave Ox_7). This assumption is consistent with the data presented in [1].

The steady-state voltammograms obtained with the stainless steel working electrode in the Li_2CO_3–K_2CO_3 and Na_2CO_3–K_2CO_3 melts are shown in Figures 3, 4 and 10. Comparison of curve a and curve b in Figure 10 shows the different anodic behaviour of stainless steel inside the potential window for the Li^+- and Na^+-containing electrolytes (waves Ox_5, Ox_9, Ox_{10}, Ox_{11}, Ox_{12}). This indicates the differences in the types of oxide layers on the surface of stainless steel in these electrolytes. It is also apparent that Li^+ and Na^+ participate in oxide layer formation. This conclusion is consistent with the data presented in [21] and [22]. According to [22], the oxide surface layer on the surface of 316 L stainless steel has the following composition: $(Fe,Ni)Cr_2O_4$; (Fe_2O_3, $LiFe_5O_8$) and $LiFeO_2$. Taking into account the standard potential data for Fe, Ni and Cr oxide formation in molten alkali carbonates [2], it would be logical to ascribe the oxidation waves at more negative potentials (Figure 10, waves Ox_9 and Ox_{11}) to the oxidation of

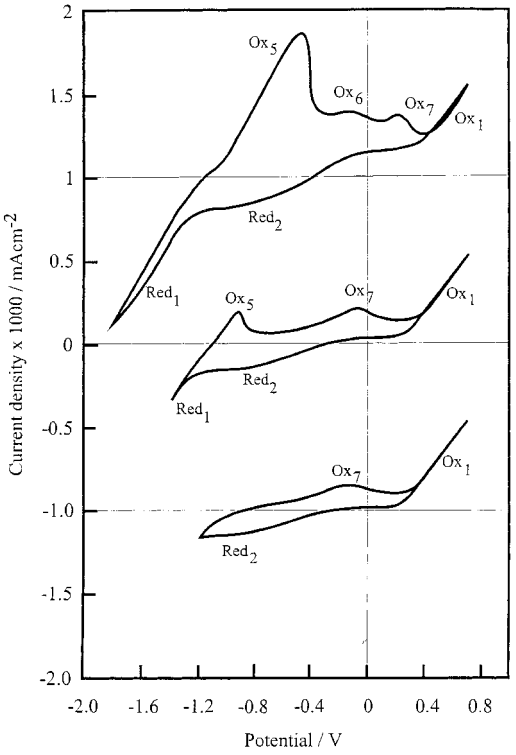

Fig. 9. Cyclic voltammetric curves obtained for a Ni electrode in Li_2CO_3–K_2CO_3 eutectic electrolyte at 650 °C and 100 mV s^{-1} in a reducing atmosphere (10% hydrogen–90% nitrogen). (NB current density in A cm^{-2}).

iron. Waves Ox_{10} and Ox_{12} (Figure 10) can be attributed to anodic dissolution of Cr or Ni components of stainless steel. As for the nickel electrode, it can be assumed that wave Ox_5 (Figure 10, curve a) obtained at the stainless steel electrode in the Li_2CO_3–K_2CO_3 melt corresponds to electrochemical oxidation of hydrogen. This is an electrocatalytic reaction and is therefore sensitive to the nature of the electrode material or the surface oxide layer. This reaction can explain the difference in anodic behaviour of the stainless steel electrode in the Li_2CO_3–K_2CO_3 and Na_2CO_3–K_2CO_3 melts (compare curves a and b in Figure 10). Figure 11 shows the electrochemical behaviour of stainless steel in the Li_2CO_3–K_2CO_3 melt during steady-state voltammetric cycling. It can be seen that the corrosion resistance of the stainless steel decreases during cycling; the passivation peaks Ox_9 and Ox_{10} grow during cycling and move to more positive potentials. As with the nickel electrode and consistent with [21], we can assume that the waves Red_3 and Red_4 (Figure 8) are due to the reduction of the surface oxide layers formed during the reactions Ox_9 and Ox_{10} (Figure 8).

The electrochemical behaviour of the Cr- and CrN-coated stainless steel electrodes during the steady-state voltammetric cycling is illustrated in Figures 5 and 6. Unlike the unprotected stainless steel, Cr- and CrN-coated electrodes improve with respect to corrosion protection during cycling; the anodic reactions inside the electrochemical stability window for the electrolyte (Ox_{12} and Ox_{13}) are suppressed after the first cycle. According to [20], Reaction 4 (Figure 5, wave Ox_4) limits the potential window for the corrosion stability of chromium. However, it can be seen from the data in Figure 5, that precycling of the Cr- and CrN-coated electrodes at potentials more positive than the potential of wave Ox_4 can efficiently improve the corrosion protection properties of these surface coatings (Figures 5 and 6). Comparison of the voltammetric data presented in Figures 5, 6 and 11 shows that the waves Ox_{12} and Ox_{13} (Figures 5, 6) are most likely due to the anodic dissolution of stainless steel through the pores in the surface coatings, with formation of mixed Fe, Ni and Cr oxides [22] (Figure 11, waves Ox_{10} and Ox_{11}). During the first cycles, these corrosion products can fill up the

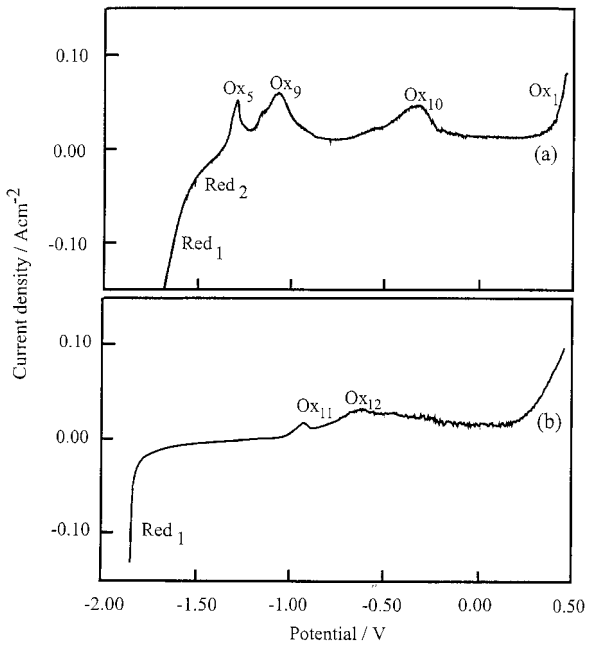

Fig. 10. Steady-state voltammetric curves obtained for the stainless steel electrode (316L) (a) in Li_2CO_3–K_2CO_3 eutectic electrolyte at 650 °C and (b) in Na_2CO_3–K_2CO_3 (62–38 mol %) electrolyte atmosphere at 730 °C and 1 mV s^{-1} in a reducing atmosphere (10% hydrogen–90% nitrogen).

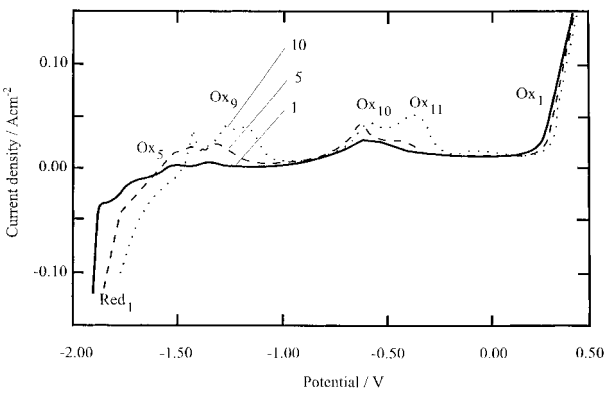

Fig. 11. Electrochemical behaviour of stainless steel (316L) during repeated steady-state voltammetric polarization in Li_2CO_3–K_2CO_3 eutectic electrolyte at 650 °C and 1 mV s^{-1} (1st–10th runs) in a reducing atmosphere (10% hydrogen–90% nitrogen).

pores and in this way increase the corrosion resistance of the Cr and CrN coatings. The degree of improvement should clearly depend on the number and size of the pits and other defects in the Cr and CrN coatings.

The voltammetric data obtained with a titanium electrode in the Li_2CO_3–K_2CO_3 and Na_2CO_3–K_2CO_3 melts are given in Figures 12 and 13. In the Li_2CO_3–K_2CO_3 melt (Figure 12), the anodic waves Ox_{14} and Ox_{15} appear inside the potential window (of electrochemical stability of the electrolyte) during the first cycle. Taking into account the data given in [18, 24] it can be assumed that wave Ox_{14} is due to electrochemical dissolution of Ti with formation of a Li_2TiO_3 surface layer, and wave Ox_{15} is due to partial Li^+ deintercalation from this layer. In contrast to the Cr- and CrN-coated electrodes, there is no significant improvement in corrosion properties of the titanium electrode during the voltammetric cycling: wave Ox_{14} disappears, but wave Ox_{15} increases. It can be seen from Figures 12 and 13 that Li^+ and Na^+ ions indeed participate in the formation of the oxide layer at the titanium electrode, since the parameters for the anodic waves depend strongly on the cationic composition of the electrolyte (compare waves Ox_{14}, Ox_{15} in Figure 13 and Ox_{16} in Figure 13). Moreover, it is clear from Figures 12 and 13 that the Li-containing oxide layer confers better corrosion protection than the Na-containing oxide layer.

The electrochemical behaviour of the TiN-coated stainless steel electrode is demonstrated in Figure 14. It is apparent that the voltammetric characteristics observed for the TiN-coated electrode differ from the voltammetric characteristics for the Ti electrode (Figure 12). This can be explained on the basis of the difference in composition of the surface layers on these electrodes. Moreover, a comparison of Figures 14 and 11 shows the identity of waves Ox_{10}, Ox_{11} and waves Ox_{17}, Ox_{18}. This implies that while TiN itself has high corrosion stability (no anodic waves due to TiN dissolution), the TiN coating must have a lot of pits and other defects through which dissolution by corrosion of the stainless steel proceeds. This conclusion is

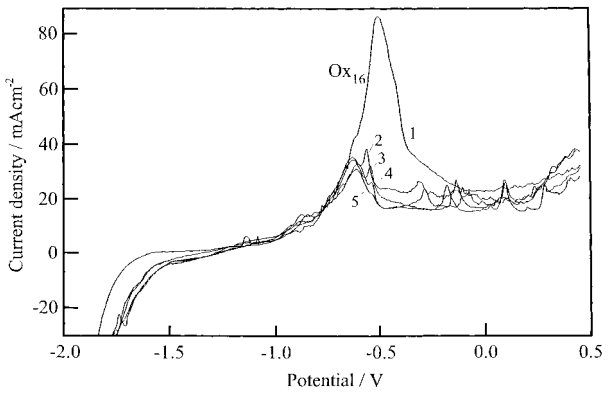

Fig. 13. Electrochemical behaviour of Ti during the repeated steady-state voltammetric polarization in Na_2CO_3–K_2CO_3 (62–38 mol %) electrolyte at 730 °C and 1 mV s^{-1} (1st–5th runs) in a reducing atmosphere (10% hydrogen–90% nitrogen).

consistent with the data obtained for the TiN-coated stainless steel before and after the corrosion test using SEM and EDX techniques (see Figure 15 and Table 1). It can be seen from Figure 16 that the TiN coating indeed has microdefects. Table 1 and Figure 15(b) and (c) show that there is a noticeable change in the composition and crystal structure of the surface layer after the corrosion test in molten Li_2CO_3–K_2CO_3. There is a significant decrease in the concentration of Ti, and an increase in the concentration of the main components of stainless steel, that is, Fe, Cr and Ni. It can therefore be assumed that waves Ox_{17} and Ox_{18} (Figure 14) represent the dissolution of stainless steel through the pits and other defects in the TiN coating with the formation of a mixed oxide layer ($(Fe,Ni)Cr_2O_4$) [22].

The results of the SEM and EDX investigation of the TiN-coated stainless steel after the corrosion test in the Na_2CO_3–K_2CO_3 melt are shown in Figure 15 and Table 1. Comparison of (a) and (c) in Figure 15 (and also data in Table 1) shows that alkali metal cations also participate in the formation of this oxide layer. Moreover, Li^+ and Na^+ participation defines the structure (Figure 15(a) and (b)) and composition of the surface

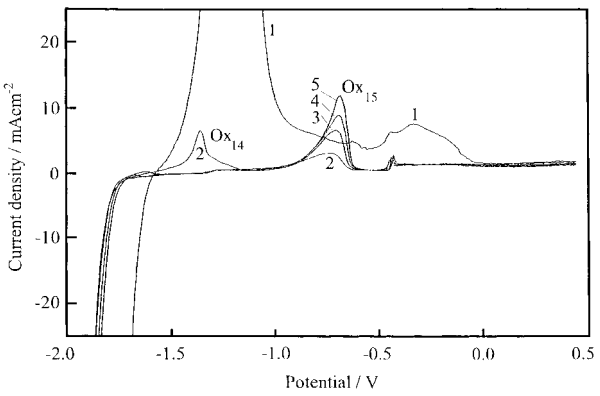

Fig. 12. Electrochemical behaviour of Ti during the repeated steady-state voltammetric polarization in Li_2CO_3–K_2CO_3 eutectic electrolyte at 650 °C and 1 mV s^{-1} (1st–5th runs) in a reducing atmosphere (10% hydrogen–90% nitrogen).

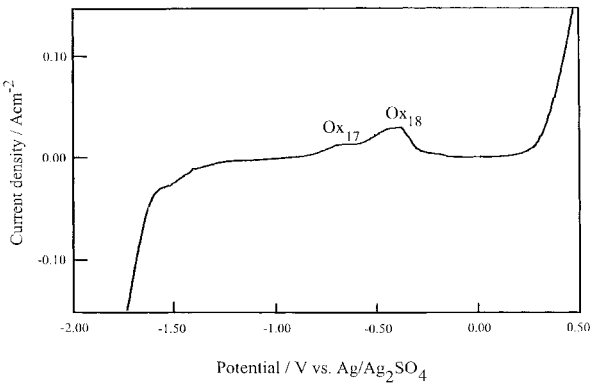

Fig. 14. Steady-state voltammetric curve obtained for a TiN-coated stainless steel (316L) electrode in Li_2CO_3–K_2CO_3 eutectic electrolyte at 650 °C and 1 mV s^{-1} (1st run) in a reducing atmosphere (10% hydrogen–90% nitrogen).

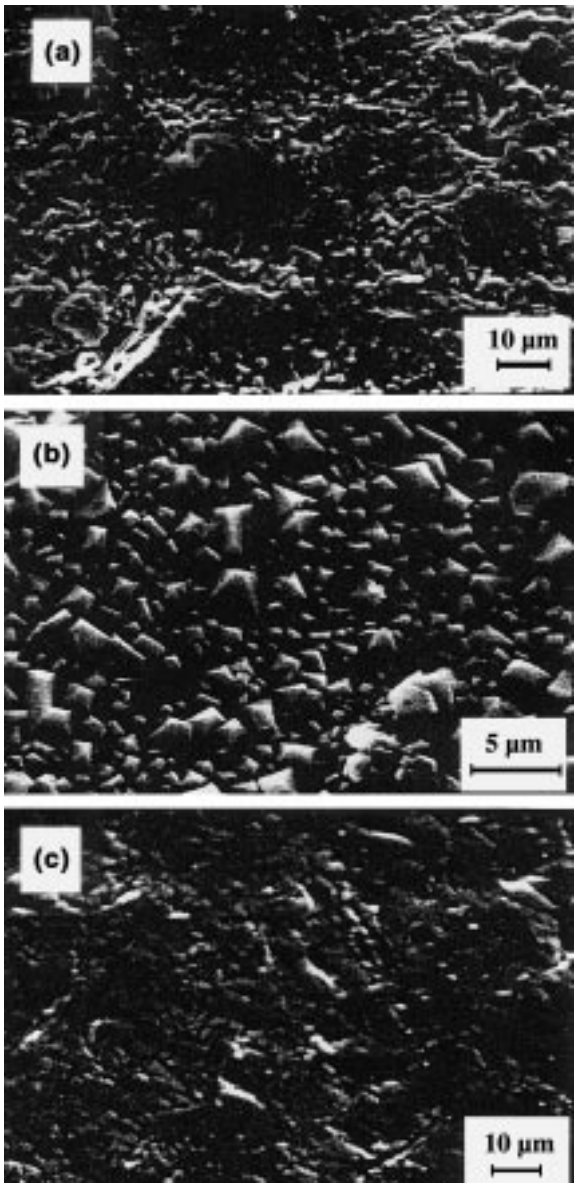

Fig. 15. Surface of the TiN-coated stainless steel (316L) sample (a) after 24 h of corrosion test in Na_2CO_3–K_2CO_3 (62–38 mol %) electrolyte at 730 °C in a reducing atmosphere (10% hydrogen–90% nitrogen), (b) after 24 h of corrosion test in Li_2CO_3–K_2CO_3 eutectic electrolyte at 650 °C in a reducing atmosphere (10% hydrogen–90% nitrogen); (c) before the corrosion test.

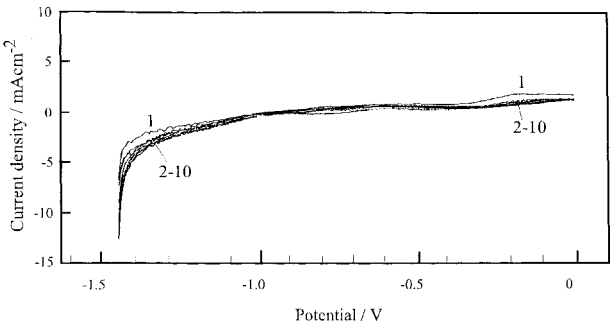

Fig. 16. Electrochemical behaviour of the TiN–AlN-coated stainless steel (316L) electrode during repeated steady-state voltammetric polarisation in Li_2CO_3–K_2CO_3 eutectic electrolyte at 650 °C and 1 mV s^{-1} (1st–10th runs) in a reducing atmosphere (10% hydrogen–90% nitrogen).

oxide layer (Table 1). It can also be seen that in the Li-containing melt, the surface oxide layer has a higher concentration of Ti and Cr than in the Na-containing melt. This could imply a higher corrosion resistance of TiN-coated stainless steel in molten Li_2CO_3–K_2CO_3 than in molten Na_2CO_3–K_2CO_3. It can also be concluded that the corrosion resistance of the TiN coatings will depend strongly on the coating technique, which defines the number of pits and other defects. This conclusion is consistent with the better corrosion test results for a TiN–Ti_2N coating obtained by chemical vapour deposition (CVD) [17].

The steady-state voltammogams obtained at the AlN–TiN-coated stainless steel electrode in the molten Li_2CO_3–K_2CO_3 are shown in Figures 4 and 16. No waves attributable to anodic electrochemical processes are visible inside the stability potential window for the electrolyte, especially when the voltammetric cycling occurs at negative potentials (Figure 16). This shows AlN–TiN to be a promising surface corrosion protective layer for the cathodic compartment of MCFC.

4. Conclusions

AlN–TiN coatings demonstrated the best corrosion resistance among the materials studied. Moreover, the

Table 1. EDX data for the element content in the surface layers for TiN-coated stainless steel electrodes before and after corrosion tests in Li_2CO_3–K_2CO_3 (62–38 mol %) and Na_2CO_3–K_2CO_3 (62–38 mol %) melts at 650 °C and 730 °C, respectively

Element	Elements in surface layer before corrosion test /wt %	Elements in surface layer after corrosion test in Li_2CO_3–K_2CO_3 melt /wt %	Elements in surface layer after corrosion test in Na_2CO_3–K_2CO_3 melt /wt %
Ti K_α	$89_{.88}$	7.1_4	0.7_5
Fe K_α	3.5_7	$72_{.99}$	$87_{.09}$
Cr K_α	0.9_9	5.8_5	0.7_4
Ni K_α	0.6_0	11.2_4	0.2_0
K K_α		0.6_8	2.9_3
Na K_α			6.1_2
Cl K_α	4.9_6		
S K_α		0.3_0	0.2_5
Ca K_α			0.5_3
Si K_α		1.5_0	0.3_1
Mn K_α		0.2_0	0.8_3

voltammetric behaviour of these coatings is very similar to the electrochemical behaviour of gold in molten carbonates, that is, the behaviour is very different from that of pure aluminium in most of the molten salt media (Al, passivated by a low-conductive layer, usually has a very low electrochemical activity in the wide potential region [2, 19]). It implies that the protective oxide coating produced from AlN–TiN has high electronic conductivity.

CrN surface coatings exhibited high corrosion resistance over a wide potential range after the precycling. TiN itself has a high corrosion resistance, but the PVD-produced coating contains pitholes and can therefore not protect the stainless steel effectively.

The improved corrosion protection of the nitride coatings may be explained as follows: titanium, aluminium and chromium nitrides are thermodynamically less stable than the corresponding oxides in the molten alkali carbonates. After contact with the molten carbonates, nitrogen in the nitrides will therefore be exchanged for oxygen. After this exchange, N atoms will diffuse inside the stainless steel support thus reducing the interface tension and improving the adhesion between stainless steel support and surface oxide layer.

Acknowledgement

The authors are indebted to DTI (Danish Institute of Technology) for preparing PVD coatings. The Commission of the European Communities supported this work within the framework of the JOULE-II programme. The authors are also grateful to B.K. Andersen for valuable discussions.

References

1. J.P.T. Vossen, L. Plomp and J.H.W. de Wit, *J. Electrochem. Soc.* **141** (1994) 3040.
2. J.R. Selman and H.C. Maru, *in* 'Advances In Molten Salt Chemistry' vol. 4, (edited by G. Mamantov, J. Braunstein and C.B. Mamantov), (Plenum Press, New York, 1981), pp. 159–390.
3. T. Nishina, K. Yuasa and I. Uchida, Spring Meeting of the Electrochemical Society, Honolulu, Hawaii, 16–21 May, 1993. Extended Abstracts. **93-1** (1993) 1532.
4. H. Tateishi and K. Imai, *Trans. Mater. Res. Soc. Jpn.* **14A** (1994) 175.
5. Jap. Patent *JP 03025858* A*2 910204*.
6. Jap. Patent *JP 04293766* A*2 921019*.
7. Jap. Patent *JP 06260178* A*2 940916*.
8. G.V. Samsonov and I.M. Vinitskii, 'Handbook of Refractory Compounds' (IFI/Plenum, New York, 1980).
9. J.W. Schultze, N. Heide and B. Siemensmeyer, Spring Meeting of the Electrochemical Society, Honolulu, Hawaii, 16–21 May, 1993. Extended Abstracts. **93-1** (1993) 227.
10. G. Bellanger and J.J. Rameau, *Electrochim. Acta* **40** (1995) 2519.
11. I. Milosev, H.H. Strehblow and B. Navinsek, 45th Annual Meeting of the International Society of Electrochemistry, Porto (1994).
12. D.R. Stull and H. Prophet (Eds), 'JANAF Thermochemical Tables', 2nd edn, NSRDS-NBS 37, Washington, DC (1971).
13. M. Keijzer, K. Hemmes, P.J.M. van der Put, J.H.W. de Wit and J. Schoonman, *Corrosion Sci.* **39** (1997) 483.
14. N.J. Bjerrum, F. Borup, I.M. Petrushina and Li Qingfeng, Danish Patent *1082/95* (1995).
15. N.J. Bjerrum, F. Borup, I.M. Petrushina and L. Qingfeng. The Electrochemical Society Meeting Abstracts, Spring Meeting, Los Angeles, CA, 5–10 May **96-1** (1996) 1461.
16. M. Keijzer, S.F. Au, P.J.J.M. van der Put, K. Hemmes, J. Schoonman and J.H.W. de Wit, Joint International Meeting, the 192nd Meeting of The Electrochemical Society, Inc. and 48th Annual Meeting of the International Society of Electrochemistry, 31 Aug.–5 Sept. 1997, Paris, Meeting Abstracts **EA 97-2** (1997) 2506.
17. M. Keijzer, P.J.J.M. van der Put, J. Schoonman, S.F. Au, K. Hemmes and J.H.W. de Wit, *op. cit.* [16] **EA 97-2** (1997) 2666.
18. V. Chauvaut, M. Cassir and Y. Denos, *in* 'Molten Salt Chemistry and Technology' vol. 5–6 (edited by H. Wendt), (Trans Tech Publications, Switzerland, 1998), p. 143.
19. V.D. Prisyazhnyi, I.M. Petrushina, S.I. Tchernukhin and V.P. Tchernobaiev, 5th International Meeting on 'Lithium Batteries', Program and Extended Abstracts, 27 May–1 June 1990, Beijing, China, **PB-39**, p. 281.
20. J.P.T. Vossen, R.S. Makkus and J.H.W. de Wit, *J. Electrochem. Soc.* **143** (1996) 66.
21. J.P.T. Vossen, L. Plomp, J.H.W. de Wit and G. Rietveld, *J. Electrochem. Soc.* **142** (1995) 3327.
22. P. Biedenkopf, M. Spiegel and H.J. Grabke, *in op. cit.* [18], vol. 5–6, (edited by H. Wendt), p. 119.
23. W.M. Mueller, J.P. Blackledge and G.G. Libowitz, 'Metal Hydrides' (Academic Press, New York/London, 1968).
24. V. Chauvaut, M. Cassir and Y. Denos, *Electrochim. Acta* **43** (1998) 1991.